

# Identification of Epigenetically Silenced Genes in Tumor Endothelial Cells

Debby M.E.I. Hellebrekers,<sup>1</sup> Veerle Melotte,<sup>1</sup> Emmanuelle Viré,<sup>2</sup> Elise Langenkamp,<sup>3</sup> Grietje Molema,<sup>3</sup> François Fuks,<sup>2</sup> James G. Herman,<sup>4</sup> Wim Van Criekinge,<sup>5</sup> Arjan W. Griffioen,<sup>1</sup> and Manon van Engeland<sup>1</sup>

<sup>1</sup>Department of Pathology, Research Institute for Growth and Development, Maastricht University and University Hospital, Maastricht, the Netherlands; <sup>2</sup>Free University of Brussels, Faculty of Medicine, Laboratory of Molecular Virology, Brussels, Belgium;

<sup>3</sup>Department of Pathology and Laboratory Medicine, University Medical Center Groningen, University of Groningen, Groningen, the Netherlands; <sup>4</sup>The Sidney Kimmel Comprehensive Cancer Center at Johns Hopkins, Baltimore,

Maryland; and <sup>5</sup>Laboratory of Bioinformatics and Computational Genomics, Department of Molecular Biotechnology, Faculty of Bioscience Engineering, University of Ghent, Ghent, Belgium

## Abstract

**Tumor angiogenesis requires intricate regulation of gene expression in endothelial cells. We recently showed that DNA methyltransferase (DNMT) and histone deacetylase (HDAC) inhibitors directly repress endothelial cell growth and tumor angiogenesis, suggesting that epigenetic modifications mediated by DNMTs and HDAC are involved in regulation of endothelial cell gene expression during tumor angiogenesis. To understand the mechanisms behind the epigenetic regulation of tumor angiogenesis, we used microarray analysis to perform a comprehensive screen to identify genes down-regulated in tumor-conditioned versus quiescent endothelial cells, and reexpressed by 5-aza-2'-deoxycytidine (DAC) and trichostatin A (TSA). Among the 81 genes identified, 77% harbored a promoter CpG island. Validation of mRNA levels of a subset of genes confirmed significant down-regulation in tumor-conditioned endothelial cells and reactivation by treatment with a combination of DAC and TSA, as well as by both compounds separately. Silencing of these genes in tumor-conditioned endothelial cells correlated with promoter histone H3 deacetylation and loss of H3 lysine 4 methylation, but did not involve DNA methylation of promoter CpG islands. For six genes, down-regulation in microdissected human tumor endothelium was confirmed. Functional validation by RNA interference revealed that clusterin, fibrillin 1, and quiescin Q6 are negative regulators of endothelial cell growth and angiogenesis. In summary, our data identify novel angiogenesis-suppressing genes that become silenced in tumor-conditioned endothelial cells in association with promoter histone modifications and reactivated by DNMT and HDAC inhibitors through reversal of these epigenetic modifications, providing a mechanism for epigenetic regulation of tumor angiogenesis. [Cancer Res 2007;67(9):4138–48]**

## Introduction

Tumor angiogenesis is essential for tumor progression and the development of metastases. The angiogenic cascade starts with

activation of endothelial cells by angiogenic growth factors, resulting in extracellular matrix degradation, endothelial cell migration, proliferation and tube formation, and, eventually, maturation of the blood vessel (1). During this multistep process, angiogenic stimulation changes endothelial cell gene expression profiles. Analysis of differentially expressed genes in tumor endothelial cell versus normal, quiescent endothelium can lead to a better understanding of endothelial cell biology during tumor angiogenesis and to the identification of tumor endothelial cell-specific markers for vascular targeting approaches (2–4).

Epigenetic processes play a major role in regulation of gene expression by affecting chromatin structure. DNA methylation and histone modifications are important mediators of epigenetic gene silencing and are essential in diverse biological processes (5, 6). In cancer cells, aberrant promoter CpG island hypermethylation and histone modifications result in inappropriate transcriptional silencing of tumor-suppressor genes (7). DNA methyltransferase (DNMT) and histone deacetylase (HDAC) inhibitors can synergistically reactivate epigenetically silenced tumor-suppressor genes and cause growth arrest and apoptosis of tumor cells (8, 9). Microarray-based strategies combining gene expression status and pharmacologic reversal of epigenetic repression have been shown powerful for identification of new epigenetically silenced tumor-suppressor genes in human cancers (10, 11).

Recently, we and others showed that DNMT and HDAC inhibitors directly inhibit endothelial cell growth and tumor angiogenesis (12–14). These findings suggest that epigenetic modifications mediated by DNMTs and HDACs are involved in regulation of endothelial cell gene expression during tumor angiogenesis. However, very little is known on the role of epigenetics in tumor endothelial cell gene expression, and on the genes regulated by DNMT and HDAC inhibitors in tumor endothelial cells. Here, we used gene expression microarrays to perform a comprehensive screen for the identification of genes silenced in tumor-conditioned endothelial cells and reexpressed by pharmacologic inhibition of DNMTs and HDACs, to provide a mechanism for the epigenetic regulation of tumor angiogenesis and for the angiostatic effects of DNMT and HDAC inhibitors.

## Materials and Methods

**Cell cultures and reagents.** Human umbilical vein endothelial cells (HUVEC) were isolated from normal human umbilical cords by perfusion with 0.125% trypsin/EDTA. HUVECs and human microvascular endothelial cells (HMEC) were cultured as previously described (15). Quiescent endothelial cells were prepared by culturing HUVECs for 3 days in culture medium supplemented with low amounts (2%) of serum (4). Tumor

**Note:** Supplementary data for this article are available at Cancer Research Online (<http://cancerres.aacrjournals.org/>).

D.M.E.I. Hellebrekers and V. Melotte contributed equally to this work.

**Requests for reprints:** Manon van Engeland, Department of Pathology, Research Institute for Growth and Development, Maastricht University and University Hospital, P.O. Box 616, 6200 MD Maastricht, the Netherlands. Phone: 31-43-3874622; Fax: 31-43-3876613; E-mail: m.vanengeland@path.unimaas.nl.

©2007 American Association for Cancer Research.

doi:10.1158/0008-5472.CAN-06-3032

conditions were mimicked by a 6-day exposure to the angiogenic growth factors basic fibroblast growth factor (bFGF; Peprotech) and vascular endothelial growth factor (VEGF; Peprotech; both at 10 ng/mL), to mimic the angiogenic conditions in a tumor, and 20% (v/v) of a 1:1 mixture of filtered culture supernatants of LS174T and CaCo-2 human colon carcinoma cell lines (4, 12). During the last 3 days, tumor-conditioned HUVECs were treated with low doses of the DNMT inhibitor 5-aza-2'-deoxycytidine (DAC; 200 nmol/L ref. 10; Sigma) or the HDAC inhibitor trichostatin A (TSA; 300 nmol/L ref. 10; Wako), replacing drugs and culture medium every 24 h, as described previously (10, 12). Tumor-conditioned endothelial cells treated during the last 3 days with a combination of DAC and TSA were first treated with DAC (200 nmol/L) for 48 h, with drug and medium replaced 24 h after the beginning of the treatment, followed by medium replacement and addition of TSA (300 nmol/L) for a further 24 h, as described previously (10).

**Microarrays.** A commercial pool (a mixture of 32 donors) of HUVEC (Tebu-bio) was used for DNA microarray experiments. Total RNA was isolated using the RNeasy RNA isolation kit (Qiagen) according to the supplier's protocol. Possible genomic DNA contaminations were removed by on column DNase treatment with the RNase-free DNase set (Qiagen). The purified RNA was quantified using a Nanodrop spectrophotometer, and RNA quality was evaluated using the Agilent 2100 Bioanalyzer. cDNA synthesis was done using the Agilent Fluorescent Direct Label kit with direct incorporation of either cyanine 5 (Cy5) or Cy3-dCTP nucleotides (Perkin-Elmer) according to the manufacturer's instructions. Labeled cDNA was purified using QIAquick PCR purification columns (Qiagen), followed by concentration by vacuum centrifugation. The Agilent human 1A cDNA microarray (Agilent Technologies) contained ~15,000 cDNA probes. Labeled cDNA was resuspended in hybridization buffer and hybridized to Agilent human 1A cDNA microarray for 17 h at 65°C, according to the Agilent protocols. All hybridizations were replicated with cyanine dyes switched. Two fluorescent microarray comparisons were done: (a) a comparison of tumor-conditioned HUVEC and quiescent HUVEC and (b) a comparison of tumor-conditioned HUVEC treated with or without a combination of DAC and TSA.

**Microarray data processing and statistical analysis.** The image file was processed using Agilent's Feature Extraction software (version A.6.1.1, Agilent Technologies). This Feature Extraction program was used to identify pixels corresponding to fluorescent signal (as opposed to background) and to remove pixels with intensities that met the default criteria for outliers. The different normalization routines applied [local background, minimum signal (feature or background), and average of all background areas] resulted in comparable results. For each identified area of signal and each of the two dyes, the basic measure of RNA abundance was taken to be the mean intensity over pixels in the identified signal area. The log ratio of the red to green intensities for each signal area was used for statistical analyses, with all subsequent analyses done using the R statistical software package (version 1.2). We selected fold-change 1.5 as a threshold because the four hybridizations increase the likelihood of statistical reliability.

**Quantitative real-time reverse transcription-PCR.** To validate microarray results, total RNA isolation, cDNA synthesis, and quantitative real-time reverse transcription-PCR (RT-PCR) of four independent HUVEC cultures were done essentially as described previously (16) using SYBR green PCR master mix (Applied Biosystems). Primer sequences are listed in Supplementary Table S1. To analyze gene expression in human tissue, endothelial cells were laser microdissected from 5 µm cryosections of frozen human colon carcinoma and normal human colon tissue using the Laser Robot Microbeam System (P.A.L.M. Microlaser Technology AG). Based on morphologic appearance in hematoxylin stained sections, ~700,000 and 1,500,000 µm<sup>2</sup> surface area of microvascular endothelium (from tumor and normal colon, respectively) was dissected per tissue. RNA extraction from the dissected cells was done according to the protocol of Absolutely RNA Microprep kit (Stratagene). Endothelial enrichment of microdissected samples was determined by comparing CD31 mRNA levels (Hs00169777\_m1, Applied Biosystems) in whole tissue RNA isolates and in microdissected materials, yielding a 24- and 60-fold enrichment factor for tumor and normal colon endothelium, respectively.

**Bisulfite sequencing.** Genomic DNA from tumor-conditioned and quiescent HUVEC [prepared from a commercial pool ( $n = 32$ ) of HUVEC; Tebu-bio] was isolated using the Puregene DNA Isolation Kit (Gentra Systems, Biozym, Landgraaf, the Netherlands). Bisulfite modification of genomic DNA and bisulfite sequencing was carried out essentially as described previously (12). Primer sequences are listed in Supplementary Table S2.

**Chromatin immunoprecipitation assay.** Chromatin immunoprecipitation (ChIP) assays were done essentially as described (17) using anti-acetyl-histone H3 (Lys<sup>9</sup> and Lys<sup>14</sup>) or anti-trimethyl-histone H3 (Lys<sup>4</sup>) antibody (both from Upstate Biotechnology). See Supplementary Methods and Supplementary Table S3 for more information and primer sequences.

**Short hairpin RNA.** For transient knockdown of *clusterin*, *fibrillin 1*, and *quiescin Q6*, a 72-bp DNA sequence encoding a short hairpin RNA (shRNA), was inserted into the pRNAT-U6.1/hygro/green fluorescent protein (GFP) expression vector (Genscript). For each gene, a shRNA was designed using the siRNA construct builder (Genscript) and purchased by Eurogentec (sequences are listed in Supplementary Table S4). Due to the limited lifespan of primary HUVEC, an endothelial cell line (HMEC) was used for siRNA transfections. One microgram of plasmid DNA was transfected into  $1 \times 10^6$  HMECs with the Nucleofector system (Amaxa), using the T20 protocol according to the manufacturer's instructions. After 72 h, viable and GFP-positive cells were purified by fluorescence-activated cell sorting (FACS), obtaining 98% GFP-positive cells. Gene knockdown of purified siRNA constructs and empty pRNAT-U6.1/hygro/GFP vector (control constructs) was examined by quantitative real-time RT-PCR, and subsequently used for angiogenesis assays.

**Proliferation and migration measurement.** Endothelial cell proliferation was measured using a [<sup>3</sup>H]thymidine incorporation assay as described previously (12, 18). HMECs were seeded at 5,000 cells per well in a 96-well plate and cultured for 3 days. During the last 6 h of the assay, the culture was pulsed with 0.3 µCi [methyl-<sup>3</sup>H]thymidine (Amersham Life Science) per well. Activity was measured using liquid scintillation. Three independent experiments were done and in each experiment; measurements were done in triplicate. Migration of endothelial cells was measured using the wound assay (18). In brief, confluent monolayers of HMECs were wounded using the blunt end of a glass pipette. Cultures were washed and medium was replaced. Wound width was measured in triplicate cultures at four predefined locations at start and at 2, 4, 6, and 8 h after wounding.

**In vitro angiogenesis.** After harvesting, HMECs were grown in Petri dishes for 24 h to form spheroids. Next, the spheroids were placed in a three-dimensional collagen gel containing in 8 volumes of vitrogen-100 (Collagen), 1 volume 10× concentrated α-MEM (Life Technologies), 1 volume of 11.76 mg/mL sodium bicarbonate, and 20 ng/mL bFGF. This mixture (100 µL) was suspended to each well of a 96-well culture plate, after which gelation was allowed to take place at 37°C. After gelation, medium was applied on top of the gel containing 20 ng/mL bFGF and 30 ng/mL VEGF. After 24 h, the relative increase in diameters of the spheroids was measured in two directions.

**Statistical analyses.** All values are given as mean values ± SE. Statistical analyses of the quantitative real-time RT-PCR, ChIP assay, as well as the proliferation, migration, and sprouting assays were done using the Wilcoxon-Mann-Whitney rank sum test, which was done in SPSS 10.0.5. software. All values are two-sided and  $P$  values <0.05 were considered statistically significant.

## Results

**Identification of genes reactivated by DAC and TSA in tumor-conditioned endothelial cells.** Tumor endothelial cells were mimicked using tumor-conditioned HUVECs (a commercial pool of a mixture of 32 donors), and quiescent endothelial cells were prepared by culturing HUVEC under low serum conditions (4, 12). For inhibition of DNMT and HDAC activity, cells were exposed to low dose (200 nmol/L) of the DNMT inhibitor DAC for 48 h, followed by treatment with 300 nmol/L of the HDAC inhibitor

TSA for a further 24 h, a method previously used to reactivate epigenetically silenced genes in tumor cells (10) and endothelial cells (12). To identify genes silenced in tumor endothelial cells by epigenetic mechanisms, we did two microarray comparisons. Combining these microarrays enabled us to select transcripts that were down-regulated in tumor-conditioned versus quiescent endothelial cells as well as reexpressed by pharmacologic treatment (Fig. 1). Both comparisons were replicated with Cy3 and Cy5 dyes switched, obtaining four separate log ratios for each cDNA probe. An expression difference of 1.5-fold was used as a threshold for all four hybridizations, thereby increasing statistical reliability. Microarray analysis revealed 86 transcripts, corresponding to 81 unique genes, that showed 1.5-fold and greater down-regulation in tumor-conditioned versus quiescent endothelial cells, as well as reactivation by DAC and TSA treatment (Table 1). Remarkably, 77% of these genes harbored a 5' CpG island (GC content >60%, ratio of observed CpG/expected CpG >0.6 and minimum length 200 bp; ref. 19) around the transcription start site or near upstream region, which is significantly more than expected from the genome-wide average of 60% (20) applied to the ~15,000 genes from our microarray ( $P < 0.0001$ ). Interestingly, 21 of 81 genes (26%) have been reported to be epigenetically silenced in the malignant cells of different tumor types (listed in Supplementary Table S5).

Changes in gene expression detected by microarray analysis were verified by quantitative real-time RT-PCR in four independent HUVEC cultures. Out of the 81 genes identified, the nine CpG island-containing genes with highest differential expression were investigated and, in addition, 20 randomly chosen genes. For 24 of these genes, significant down-regulation in tumor-conditioned versus quiescent endothelial cells was confirmed using mean relative expression values of the four HUVEC cultures (1.5- to 800-fold suppression,  $P < 0.05$ ; Fig. 2A). Validating reactivation of the selected genes in tumor-conditioned endothelial cells by treatment with a combination of DAC and TSA, as well as by both compounds separately, revealed that for 25 of the 29 (86%) genes, significant up-regulation in tumor-conditioned endothelial cells by treatment with the drug combination was confirmed, ranging from 1.5-fold (*IL6*) to 66-fold (*NPPB*) relative induction (Fig. 2B). Among these 25 genes, 24 were also significantly reactivated by TSA alone and 22 were reactivated by DAC alone. Four of the five genes (*SMTN*, *FABP4*, *USF1*, and *MCM7*) that were not (significantly) down-regulated in tumor-conditioned endothelial cells were also not significantly induced by DAC and TSA in the four HUVEC cultures (although *FABP4* was induced by the combination, it was not induced by DAC or TSA alone), indicating that the identification of these genes results from microarray background. Interestingly, most of the genes showed much stronger relative induction after treatment with TSA (ranging from 1.5- to 498-fold induction) compared with DAC (ranging from 1.3- to 8.5-fold). Comparison of relative up-regulation by the combination treatment with either compound alone showed neither an additive nor a synergistic effect for most genes. Moreover, relative induction by treatment with TSA alone was for most genes greater than by the combination treatment (Fig. 2B). Together, quantitative real-time RT-PCR confirmed the results of both microarray comparisons.

**Silencing of the identified genes in tumor-conditioned endothelial cells is associated with promoter histone modifications but not DNA methylation.** The restored expression of the selected genes by inhibition of DNMTs and HDACs suggests that epigenetic modifications mediated by these enzymes might be

responsible for silencing of these genes in tumor endothelial cells. Therefore, we examined promoter DNA methylation and histone modifications in the transcription start site area and near upstream region of the CpG islands of *clusterin* (*CLU*), *intercellular adhesion molecule 1* (*ICAM1*), *insulin-like growth factor binding protein 3* (*IGFBP3*), *fibrillin 1* (*FBNI*), *tetraspanin 2* (*TSPAN2*), *tumor necrosis factor receptor superfamily, member 21* (*TNFRSF21*), and *quiescin Q6* (*QSCN6*). These genes were selected based on (a) the presence of a promoter CpG island, (b) relative up-regulation by DAC and TSA, and (c) evidence from literature of silencing by promoter methylation, thereby choosing the most likely candidates for DNA methylation. *ICAM1*, *IGFBP3*, *FBNI*, *TSPAN2*, and *QSCN6* were described to be silenced by promoter DNA hypermethylation (*ICAM1*, *IGFBP3*, *FBNI*, and *TSPAN2*) and histone deacetylation (*QSCN6*) in tumor cells (Supplementary Table S5). In addition, *CLU* is reported to be hypermethylated in transformed rat fibroblasts (21). We also included a gene not described to be hypermethylated (*TNFRSF21*). DNA methylation of the promoter CpG islands of the selected genes was evaluated by genomic bisulfite sequencing. Interestingly, almost no methylated CpG sites were present in the promoters of *CLU*, *FBNI*, *TSPAN2*, *TNFRSF21*, and *QSCN6* in tumor-conditioned or quiescent endothelial cells (Fig. 3A). Promoter CpG islands of *ICAM1* and *IGFBP3* contained some methylated CpGs, but did not show major differences in methylation patterns between quiescent and tumor-conditioned endothelial cells. As a positive sequencing control for CpG methylation in endothelial cells, we did bisulfite sequencing of the inducible nitric oxide synthase promoter (22), which revealed dense methylation in both tumor-conditioned and quiescent endothelial cells (data not shown). To examine whether the genes become hypermethylated at later time points, we also studied promoter DNA methylation in tumor-conditioned endothelial cells after 3 weeks of stimulation. Similar to 6 days activation, hardly any methylation was found in these cells (Supplementary Data 1). These results show that despite their reactivation by DAC, silencing of the selected genes in tumor-conditioned endothelial cells occurs without changes in promoter DNA methylation in the regions examined. It is interesting that silencing of *CLU*, *ICAM1*, *IGFBP3*, *FBNI*, and *TSPAN2* in tumor cells occurs by promoter DNA methylation, whereas the same genes are silenced in tumor-conditioned endothelial cells without methylation changes. Moreover, the examined promoter regions of these

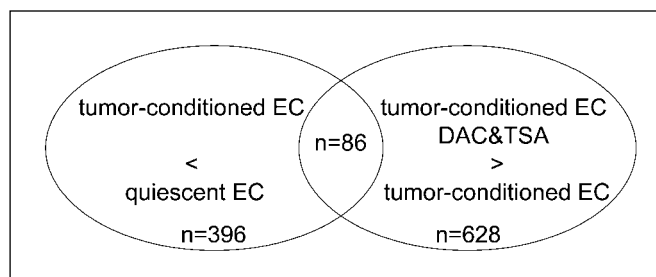


**Figure 1.** Identification of genes reactivated by DAC and TSA in tumor-conditioned endothelial cells. Two microarray comparisons were done: a comparison of tumor-conditioned versus quiescent endothelial cells (EC), and a comparison of tumor-conditioned endothelial cells treated with or without DAC and TSA. Using fold-change 1.5 as a threshold, 396 transcripts were identified as down-regulated in tumor-conditioned versus quiescent endothelial cells, and 628 transcripts were activated by DAC and TSA. Combining these microarrays revealed 86 transcripts down-regulated in tumor-conditioned versus quiescent HUVEC as well as reexpressed by pharmacologic treatment, corresponding to 81 unique genes.

**Table 1.** Genes down-regulated in tumor-conditioned endothelial cells and up-regulated by DAC and TSA

Accession no.	Gene name	Symbol	Log ratio*				Sum	Function	CpG island <sup>†</sup>
			1	2	3	4			
M64722	<i>Clusterin</i>	<i>CLU</i>	1.11	-1.21	-1.27	0.86	4.45	Apoptosis	Yes
Y13492	<i>Smoothelin</i>	<i>SMTN</i>	1.01	-0.82	-1.15	0.78	3.77	Cytoskeleton	Yes
M25296	<i>Natriuretic peptide precursor B</i>	<i>NPPB</i>	0.59	-0.44	-1.18	1.24	3.44	Hormone	Yes
U21943	<i>Solute carrier organic anion transporter family, member 1A2</i>	<i>SLCO1A2</i>	1.03	-1.11	-0.49	0.38	3.01	Metabolism	No
U81234	<i>Chemokine ligand 6</i>	<i>CXCL6</i>	0.55	-0.46	-0.77	0.68	2.46	Cytokine	Yes
M24283	<i>Intercellular adhesion molecule 1, human rhinovirus receptor</i>	<i>ICAM1</i>	0.58	-0.44	-0.68	0.47	2.17	Receptor	Yes
M59807	<i>Interleukin 32</i>	<i>IL32</i>	0.64	-0.78	-0.45	0.29	2.17	Cytokine	No
BE407364	<i>IFN, <math>\alpha</math>-inducible protein</i>	<i>GIP3</i>	0.52	-0.55	-0.61	0.49	2.17	Unknown	No
M35878	<i>Insulin-like growth factor binding protein 3</i>	<i>IGFBP3</i>	0.52	-0.47	-0.64	0.40	2.04	Cell cycle, apoptosis	Yes
X63556	<i>Fibrillin 1</i>	<i>FBN1</i>	0.68	-0.65	-0.31	0.35	2.00	Extracellular matrix	Yes
AI140760	<i>Syndecan 4</i>	<i>SDC4</i>	0.26	-0.43	-0.74	0.54	1.97	Receptor	Yes
AW192446	<i>Uncoupling protein 2 (mitochondrial, proton carrier)</i>	<i>UCP2</i>	0.24	-0.19	-0.76	0.77	1.96	Metabolism	Yes
AI022951	<i>Immediate early response 3</i>	<i>IER3</i>	0.21	-0.50	-0.94	0.29	1.93	Apoptosis	Yes
NM_001511	<i>Chemokine ligand 1</i>	<i>CXCL1</i>	0.26	-0.32	-0.73	0.58	1.89	Cytokine	Yes
M29877	<i>Fucosidase, <math>\alpha</math>-L-1, tissue</i>	<i>FUCA1</i>	0.39	-0.20	-0.64	0.64	1.88	Metabolism	Yes
AF055009	<i>Cyclic AMP responsive element binding protein 3-like 1</i>	<i>CREB3L1</i>	0.67	-0.64	-0.22	0.33	1.86	Transcription	Yes
AW269972	<i>Tetraspanin 2</i>	<i>TSPAN2</i>	0.35	-0.25	-0.64	0.54	1.79	Receptor	Yes
M59465	<i>Tumor necrosis factor, <math>\alpha</math>-induced protein 3</i>	<i>TNFAIP3</i>	0.22	-0.19	-0.66	0.72	1.79	Apoptosis	Yes
X60201	<i>Brain-derived neurotrophic factor</i>	<i>BDNF</i>	0.62	-0.59	-0.26	0.26	1.72	Growth factor	Yes
AW631118	<i>Fatty acid binding protein 4, adipocyte</i>	<i>FABP4</i>	0.34	-0.33	-0.43	0.56	1.66	Metabolism	No
X13425	<i>Tumor-associated calcium signal transducer 2</i>	<i>TACSTD2</i>	0.49	-0.57	-0.36	0.24	1.66	Receptor	Yes
M17017	<i>Interleukin 8</i>	<i>IL8</i>	0.20	-0.21	-0.68	0.51	1.61	Cytokine	No
AK000996	<i>Transmembrane protein 45A</i>	<i>TMEM45A</i>	0.22	-0.19	-0.56	0.61	1.59	Unknown	Yes
X57579	<i>Inhibin, <math>\beta</math>A</i>	<i>INHBA</i>	0.24	-0.42	-0.57	0.34	1.57	Growth factor	No
M17783	<i>Serpine peptidase inhibitor, clade E, member 2</i>	<i>SERPINE2</i>	0.22	-0.36	-0.57	0.41	1.57	Protein turnover	Yes
AW162025	<i>Neuronatin</i>	<i>NNAT</i>	0.31	-0.28	-0.45	0.48	1.52	Protein modification	Yes
M33882	<i>Myxovirus resistance 1, IFN-inducible protein p78</i>	<i>MX1</i>	0.46	-0.45	-0.33	0.27	1.51	Apoptosis	Yes
M59911	<i>Integrin, <math>\alpha</math>-3</i>	<i>ITGA3</i>	0.27	-0.28	-0.55	0.40	1.50	Receptor	Yes
X87241	<i>FAT tumor suppressor (Drosophila) homologue 1</i>	<i>FAT</i>	0.24	-0.18	-0.51	0.51	1.44	Receptor	Yes
AA661835	<i>Dystrophin</i>	<i>DMD</i>	0.36	-0.26	-0.28	0.54	1.43	Cytoskeleton	Yes
AK027126	<i>Argininosuccinate synthetase</i>	<i>ASS</i>	0.51	-0.42	-0.19	0.30	1.42	Protein turnover	Yes
AA302123	<i>IFN, <math>\alpha</math>-inducible protein 27</i>	<i>IFI27</i>	0.47	-0.41	-0.28	0.25	1.41	Unknown	No
AX008646	<i>Tumor necrosis factor receptor superfamily, member 21</i>	<i>TNFRSF21</i>	0.39	-0.45	-0.39	0.17	1.40	Receptor	Yes
AF007138	<i>NDRG family member 4</i>	<i>NDRG4</i>	0.26	-0.41	-0.47	0.24	1.39	Cell cycle	Yes
AB033101	<i>Filamin A interacting protein 1</i>	<i>FILIP1</i>	0.37	-0.46	-0.38	0.18	1.39	Unknown	No
X13916	<i>Low density lipoprotein-related protein 1</i>	<i>LRP1</i>	0.21	-0.55	-0.38	0.24	1.38	Metabolism	Yes
Z75668	<i>Chemokine ligand 11</i>	<i>CCL11</i>	0.57	-0.44	-0.17	0.19	1.37	Cytokine	No
NM_001299	<i>Calponin 1, basic, smooth muscle</i>	<i>CNN1</i>	0.17	-0.27	-0.54	0.36	1.34	Cytoskeleton	Yes
AK021874	<i>Transforming growth factor, <math>\beta</math>2</i>	<i>TGFB2</i>	0.44	-0.44	-0.22	0.23	1.33	Cell cycle	Yes
M95787	<i>Transgelin</i>	<i>TAGLN</i>	0.19	-0.30	-0.51	0.31	1.32	Cytoskeleton	No
NM_004385	<i>Chondroitin sulfate proteoglycan 2</i>	<i>CSPG2</i>	0.35	-0.32	-0.29	0.36	1.31	Extracellular matrix	Yes
AB017568	<i>Upstream transcription factor 1</i>	<i>USF1</i>	0.19	-0.22	-0.48	0.40	1.30	Transcription	No
X51405	<i>Carboxypeptidase E</i>	<i>CPE</i>	0.28	-0.38	-0.30	0.32	1.29	Metabolism	Yes
AK001580	<i>Leprecan-like 1</i>	<i>LEPREL1</i>	0.20	-0.23	-0.61	0.24	1.28	Unknown	Yes
AW131622	<i>Niemann-Pick disease, type C2</i>	<i>NPC2</i>	0.30	-0.30	-0.39	0.28	1.27	Metabolism	Yes

(Continued on the following page)

**Table 1.** Genes down-regulated in tumor-conditioned endothelial cells and up-regulated by DAC and TSA (Cont'd)

Accession no.	Gene name	Symbol	Log ratio*				Sum	Function	CpG island <sup>†</sup>
			1	2	3	4			
AB011109	<i>NUAK family, SNF1-like kinase 1</i>	<i>NUAK1</i>	0.18	-0.28	-0.44	0.32	1.22	Protein modification	Yes
NM_001553	<i>Insulin-like growth factor binding protein 7</i>	<i>IGFBP7</i>	0.45	-0.23	-0.19	0.35	1.22	Cell cycle	Yes
Y00081	<i>Interleukin 6 (IFN, <math>\beta</math> 2)</i>	<i>IL6</i>	0.41	-0.29	-0.22	0.29	1.21	Cytokine	No
U97276	<i>Quiescin Q6</i>	<i>QSCN6</i>	0.17	-0.27	-0.51	0.26	1.21	Cell cycle	Yes
X70340	<i>Transforming growth factor, <math>\alpha</math></i>	<i>TGFA</i>	0.28	-0.18	-0.32	0.41	1.19	Cell cycle	Yes
AJ003147	<i>Hypothetical protein LOC197350</i>		0.32	-0.42	-0.26	0.18	1.18	Unknown	UK
Y00285	<i>Insulin-like growth factor 2 receptor</i>	<i>IGF2R</i>	0.28	-0.38	-0.30	0.20	1.16	Receptor	Yes
AL117468	<i>CLIP-170-related protein</i>	<i>CLIPR-59</i>	0.29	-0.31	-0.24	0.32	1.16	Unknown	Yes
NM_001908	<i>Cathepsin B</i>	<i>CTSB</i>	0.28	-0.23	-0.32	0.33	1.15	Protein turnover	Yes
NM_006509	<i>v-Rel avian reticuloendotheliosis viral oncogene homologue B</i>	<i>RELB</i>	0.21	-0.30	-0.35	0.28	1.14	Transcription	Yes
AF039018	<i>PDZ and LIM domain protein 3</i>	<i>PDLIM3</i>	0.34	-0.25	-0.26	0.30	1.14	Cytoskeleton	Yes
NM_014333	<i>Immunoglobulin superfamily, member 4</i>	<i>IGSF4</i>	0.30	-0.24	-0.27	0.33	1.13	Receptor	Yes
X14766	<i><math>\gamma</math>-Aminobutyric acid A receptor, <math>\alpha 1</math></i>	<i>GABRA1</i>	0.27	-0.20	-0.22	0.43	1.12	Receptor	No
AW025439	<i>Growth arrest and DNA damage-inducible, <math>\alpha</math></i>	<i>GADD45A</i>	0.37	-0.19	-0.22	0.34	1.12	Apoptosis, cell cycle	Yes
X15880	<i>Collagen, type VI, <math>\alpha 1</math></i>	<i>COL6A1</i>	0.38	-0.29	-0.20	0.25	1.11	Extracellular matrix	Yes
L12579	<i>Cut-like 1, CCAAT displacement protein</i>	<i>CUTL1</i>	0.30	-0.24	-0.37	0.21	1.11	Transcription	Yes
U31201	<i>Laminin, <math>\gamma 2</math></i>	<i>LAMC2</i>	0.34	-0.24	-0.23	0.30	1.11	Extracellular matrix	No
U92971	<i>Coagulation factor II (thrombin) receptor-like 2</i>	<i>F2RL2</i>	0.19	-0.27	-0.30	0.35	1.11	Receptor	No
AL117664	<i>ABI gene family, member 3 binding protein</i>	<i>ABI3BP</i>	0.19	-0.24	-0.30	0.19	1.11	Unknown	No
U03106	<i>Cyclin-dependent kinase inhibitor 1A</i>	<i>CDKN1A</i>	0.49	-0.18	-0.19	0.28	1.05	Cell cycle	Yes
AI816415	<i>Ferritin, heavy polypeptide 1</i>	<i>FTH1</i>	0.20	-0.27	-0.39	0.22	1.04	Metabolism	Yes
AI677769	<i>EGF-like repeats and discoidin I-like domains 3</i>	<i>EDIL3</i>	0.37	-0.21	-0.18	0.27	1.04	Extracellular matrix	Yes
AK025732	<i>N-acylsphingosine amidohydrolase (acid ceramidase) 1</i>	<i>ASAHI</i>	0.38	-0.20	-0.19	0.35	1.03	Metabolism	Yes
D28480	<i>MCM7 minichromosome maintenance deficient 7</i>	<i>MCM7</i>	0.26	-0.17	-0.23	0.27	1.03	Cell cycle	Yes
S42303	<i>Cadherin 2, type 1, N-cadherin</i>	<i>CDH2</i>	0.22	-0.25	-0.37	0.24	1.02	Receptor	Yes
X05562	<i>Collagen, type IV, <math>\alpha 2</math></i>	<i>COL4A2</i>	0.26	-0.33	-0.27	0.17	1.01	Extracellular matrix	Yes
X02994	<i>Adenosine deaminase</i>	<i>ADA</i>	0.20	-0.20	-0.31	0.31	1.00	Metabolism	Yes
U34919	<i>ATP-binding cassette, subfamily G (WHITE), member 1</i>	<i>ABCG1</i>	0.26	-0.28	-0.23	0.21	1.00	Metabolism	Yes
AF201945	<i>Olfactomedin-like 3</i>	<i>OLFML3</i>	0.30	-0.27	-0.20	0.27	0.99	Unknown	No
AW131784	<i>Integral membrane protein 2B</i>	<i>ITM2B</i>	0.19	-0.21	-0.27	0.28	0.99	Receptor	Yes
AK024573	<i>Hypothetical protein FLJ20920</i>		0.29	-0.26	-0.20	0.27	0.98	Unknown	Yes
AW410427	<i>Collagen, type II, <math>\alpha 1</math></i>	<i>COL2A1</i>	0.19	-0.25	-0.26	0.18	0.98	Extracellular matrix	Yes
M12529	<i>Apolipoprotein E</i>	<i>APOE</i>	0.27	-0.29	-0.28	0.23	0.97	Metabolism	No
AB033421	<i>Dickkopf homologue 3</i>	<i>DKK3</i>	0.23	-0.26	-0.22	0.24	0.97	Cell cycle, apoptosis	Yes
NM_002117	<i>MHC, class I, C</i>	<i>HLA-C</i>	0.31	-0.27	-0.19	0.17	0.95	Receptor	Yes
S73906	<i>Adrenomedullin</i>	<i>ADM</i>	0.20	-0.24	-0.21	0.18	0.84	Hormone	Yes

\*Log ratio 1: HUVEC- versus HUVEC+; log ratio 2: HUVEC+ versus HUVEC-; log ratio 3: HUVEC+ versus HUVEC+ DAC and TSA; log ratio 4: HUVEC+ DAC and TSA versus HUVEC+. Genes are ranked in descending order according to the sum of the absolute values of the four individual log ratios. If genes were represented by multiple cDNA probes, the probe with the highest change in expression levels is shown.

<sup>†</sup> Yes, CpG island was found in the region (-1,000; +500) relative to the transcription start site. No, no CpG island was found in the region (-1,000; +500) relative to the transcription start site. UK, transcription start site is unknown.

genes were similar as the regions described to be methylated in tumor cells (except for *FBNI*, of which the exact location of promoter methylation in tumor cells is not described).

Promoter histone H3 acetylation of the seven selected genes was examined by ChIP in the region surrounding the transcription start site. Promoter acetyl-histone H3 levels were significantly decreased

in tumor-conditioned compared with quiescent endothelial cells in all seven genes, although subtle for *QSCN6* (Fig. 3B). Treatment of tumor-conditioned endothelial cells with the combination of DAC (200 nmol/L, 48 h) and TSA (300 nmol/L, last 24 h) caused a significant increase in promoter histone acetylation of the genes, correlating with their restored expression. Promoter histone

acetylation was also induced by treatment with DAC (200 nmol/L, 72 h) or TSA (300 nmol/L, 72 h) alone, although the effect was again subtle for *QSCN6* (Fig. 3B). We also examined lysine 4 methylation of histone H3, another histone modification associated with gene expression. As for histone acetylation, H3 lysine 4 methylation in the gene promoters was significantly decreased in tumor-conditioned versus quiescent endothelial cells, and increased by DAC and/or TSA, correlating with changes in gene expression (Fig. 3C). Thus, silencing of the selected genes in tumor-conditioned endothelial cells is associated with promoter histone H3 deacetylation and loss of H3 lysine 4 methylation, but not with DNA hypermethylation, and reexpression by DAC and TSA occurs in conjunction with restored histone acetylation and H3 lysine 4 methylation levels.

Transcriptional repression of *CLU*, *ICAM1*, *IGFBP3*, *FBN1*, *TSPAN2*, *TNFRSF21*, and *QSCN6* was validated in tumor-derived endothelial cells obtained from a colon tumor by laser microdissection. We confirmed significant down-regulation of these genes

in tumor endothelium versus endothelial cells microdissected from corresponding normal tissue (Fig. 4A). Furthermore, *ICAM1* promoter methylation was studied in microdissected tumor endothelial cells, but hardly any methylation was found (Fig. 4B).

**Clusterin, fibrillin 1, and quiescin Q6 negatively regulate endothelial cell growth and sprouting.** To explore the mechanism by which reactivation of the identified genes by DAC and TSA inhibits angiogenesis, functional validation of the identified genes was done. Of the seven genes selected, a role in angiogenesis is already reported for *IGFBP3* and *ICAM1*. *IGFBP3* has been described to inhibit VEGF-mediated endothelial cell growth (23) and angiogenesis (24), and *ICAM1* is an important endothelial cell adhesion molecule known to be down-regulated in tumor endothelial cells by angiogenic factors (25). Therefore, we further focused on the genes for which a clear role in angiogenesis has not been reported yet. From these five genes, we selected clusterin, for which both proangiogenic (26) and antiangiogenic (27) activities have been described, as well as two genes that have not been

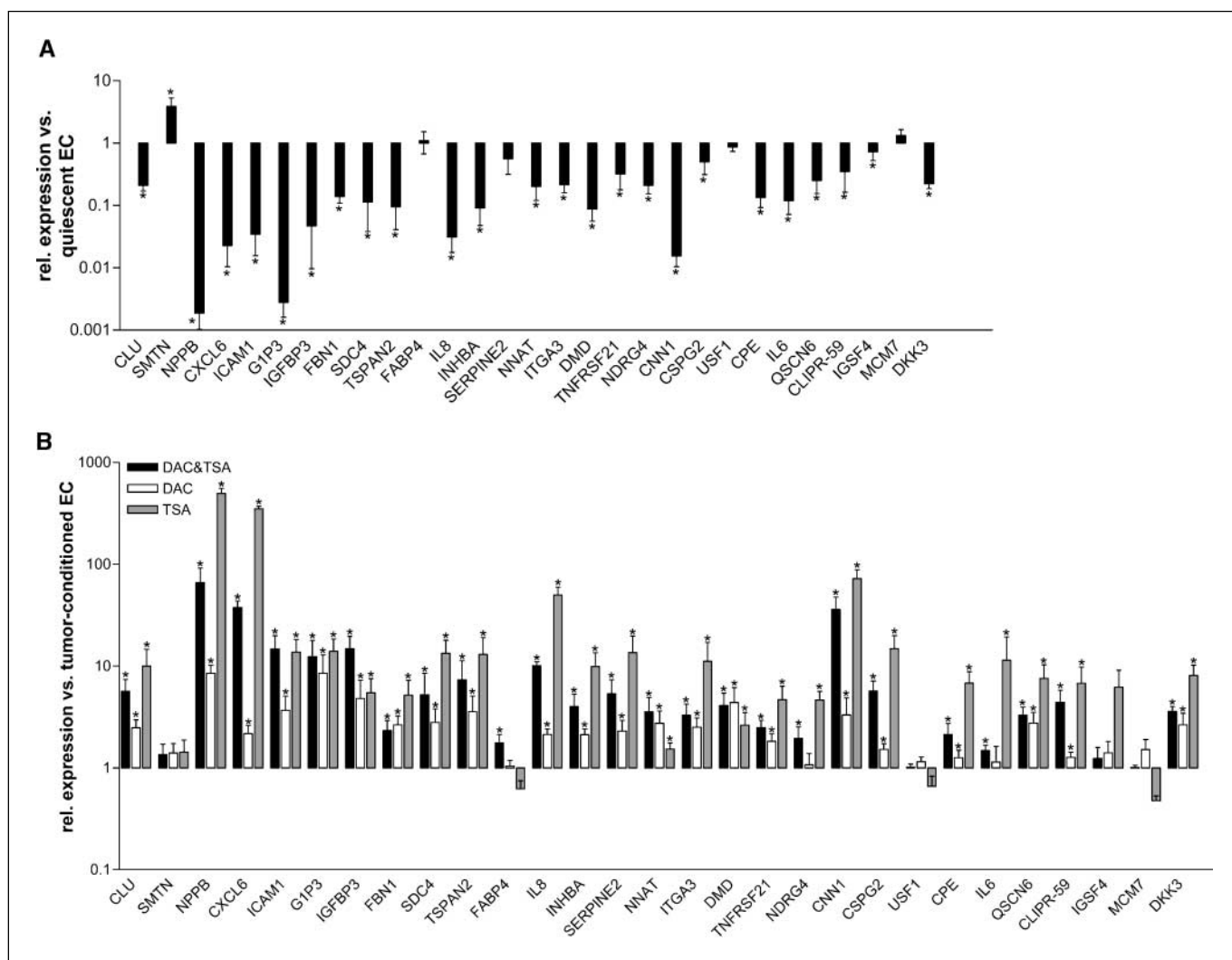


**Figure 2.** Transcriptional validation of candidate genes by quantitative real-time RT-PCR. *A*, relative mRNA expression of selected genes in tumor-conditioned versus quiescent HUVEC measured by quantitative real-time RT-PCR. Columns, mean of four independent experiments; bars, SE (\*,  $P < 0.05$  versus quiescent HUVEC). *B*, relative mRNA expression of selected genes in tumor-conditioned HUVEC treated with a combination of DAC (200 nmol/L, 48 h) and TSA (300 nmol/L, last 24 h), similar as the microarray conditions, or with DAC (200 nmol/L, 72 h) or TSA (300 nmol/L, 72 h) alone versus untreated tumor-conditioned HUVEC. Columns, mean of four independent experiments; bars, SE (\*,  $P < 0.05$  versus untreated tumor-conditioned HUVEC).

related to angiogenesis (fibrillin 1 and quiescin Q6). Effects of down-regulation of these genes on endothelial cell proliferation, migration, and sprouting were studied. To that end, HMECs were transiently transfected with GFP-labeled vectors containing shRNA targeting *CLU*, *FBN1*, or *QSCN6*, and purified by FACS. After 72 h,

shRNA treatment significantly reduced *CLU*, *FBN1*, and *QSCN6* mRNA expression when compared with cells transfected with empty pRNAT-U6.1/hygro/GFP vector (control constructs; Fig. 5A). As a further control for RNA interference specificity, we determined the expression of each gene (*CLU*, *FBN1*, and *QSCN6*) under each

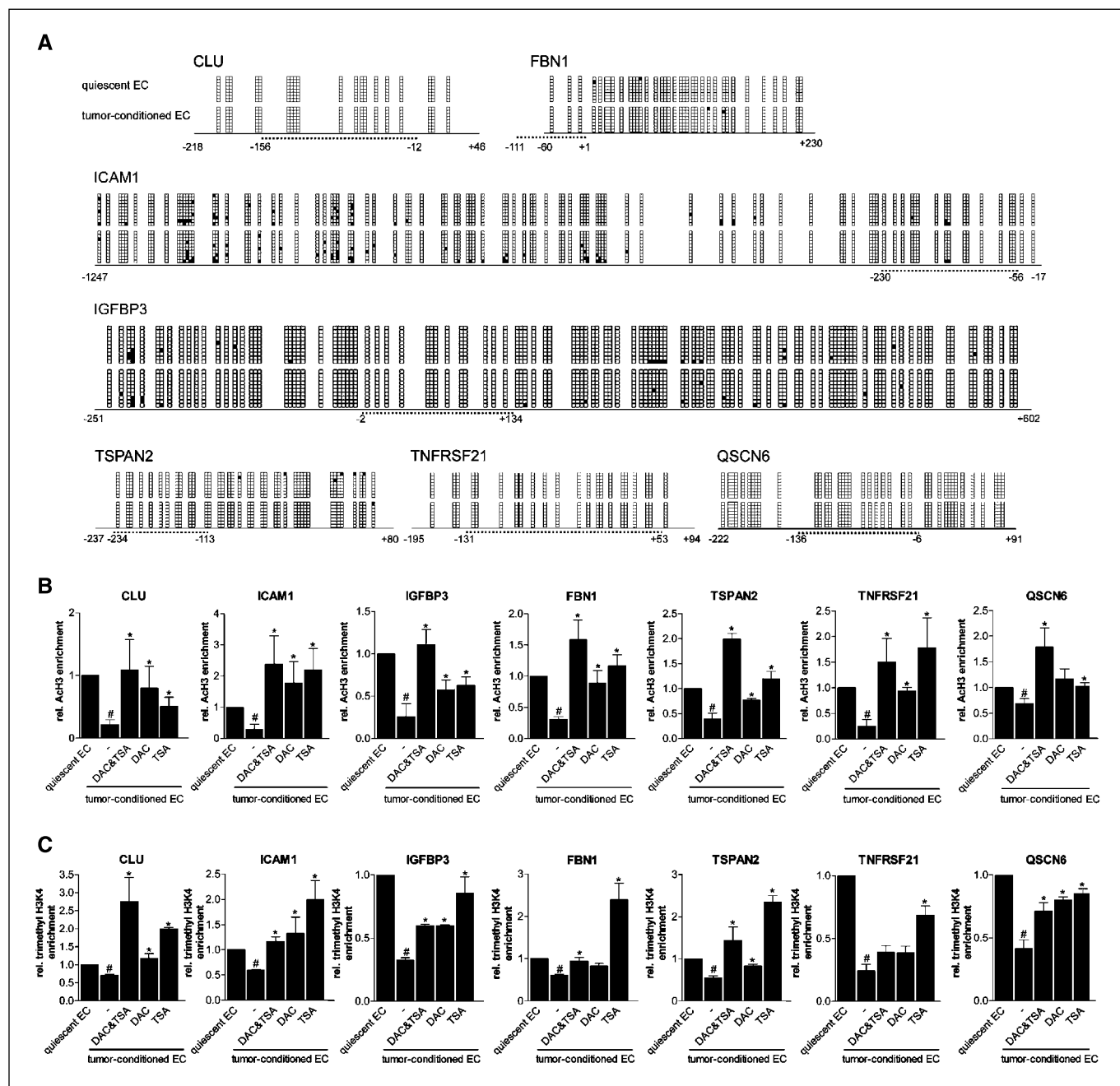


**Figure 3.** Analysis of promoter DNA methylation, histone H3 acetylation, and H3 lysine 4 methylation of candidate genes. *A*, genomic bisulfite sequencing of 5' CpG islands of *CLU*, *FBN1*, *ICAM1*, *IGFBP3*, *TSPAN2*, *TNFRSF21*, and *QSCN6* in quiescent and tumor-conditioned HUVECs. For each gene, at least eight individual clones from both quiescent and tumor-conditioned endothelial cells were sequenced. Methylation status of each CpG dinucleotide in a clone: ■, methylated; □, not methylated. *Numbers*, positions relative to the transcription start site. *Dotted lines*, regions examined by chromatin immunoprecipitation. *B* and *C*, ChIP assay using anti-acetyl-histone H3 (Lys<sup>9</sup> and Lys<sup>14</sup>; *B*) and anti-trimethyl-histone H3 (Lys<sup>4</sup>; *C*) antibody in quiescent HUVEC, tumor-conditioned HUVEC, and tumor-conditioned HUVEC treated with a combination of DAC (200 nmol/L, 48 h) and TSA (300 nmol/L, last 24 h), similar as the microarray conditions, or with DAC (200 nmol/L, 72 h) or TSA (300 nmol/L, 72 h) alone. *Dotted lines in (A)*, locations of the PCR fragments done on DNA recovered from ChIP experiments. PCR was done on nonimmunoprecipitated (input) DNA, immunoprecipitated DNA, and a no-antibody control DNA. Enrichment was calculated by taking the ratio between the net intensity of the candidate gene PCR product and the net intensity of the glyceraldehyde-3-phosphate dehydrogenase PCR product for immunoprecipitated DNA and dividing this by the same ratio calculated for the input DNA. Relative acetylated H3 (*ACh3*) and methylated H3 Lys 4 (*trimethyl H3K4*) enrichment (quiescent HUVEC set to 1). *Columns*, mean enrichment values from several independent ChIP experiments; *bars*, SE (#, *P* < 0.05 versus quiescent HUVEC; \*, *P* < 0.05 versus untreated tumor-conditioned HUVEC).

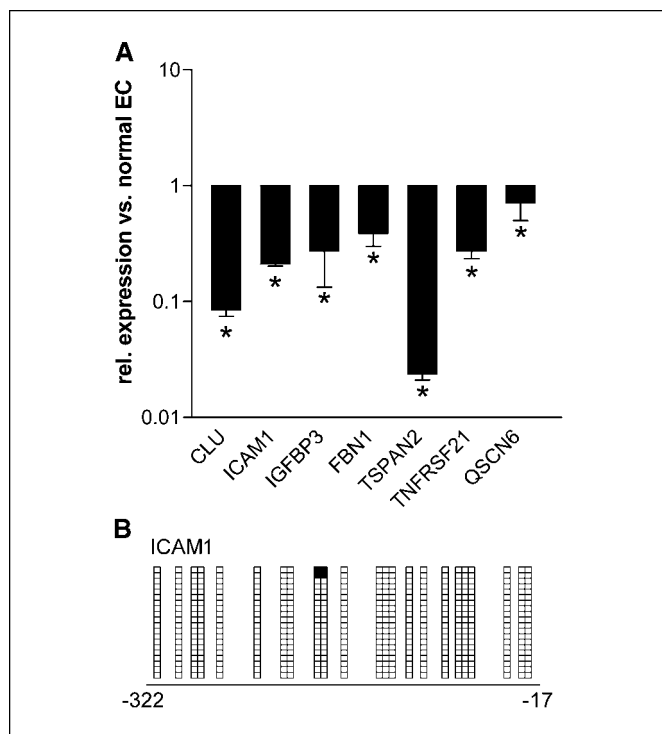


**Figure 4.** Transcriptional validation of candidate genes and ICAM1 promoter DNA methylation analysis in tumor endothelium. **A**, relative mRNA expression of *CLU*, *FBN1*, *ICAM1*, *IGFBP3*, *TSPAN2*, *TNFRSF21*, and *QSCN6* in microdissected tumor endothelium versus endothelial cells microdissected from corresponding normal tissue measured by quantitative real-time RT-PCR. Columns, mean; bars, SE (\*,  $P < 0.05$  versus normal endothelial cells). **B**, genomic bisulfite sequencing of part of the *ICAM1* promoter (-322 to -17) in tumor endothelium obtained from colorectal tumors by laser microdissection.

shRNA condition, showing that *CLU*, *FBN1*, and *QSCN6* shRNA constructs only decrease expression of their corresponding gene (Supplementary Data 2). Proliferation of endothelial cells was significantly induced upon down-regulation of *CLU*, *FBN1*, or *QSCN6* (34%, 53%, and 67% induction by *CLU*, *FBN1*, and *QSCN6* shRNA, respectively), indicating that these genes inhibit endothelial cell growth (Fig. 5B). Treatment with *CLU* shRNA showed a small but significant stimulatory effect on the migration rate of endothelial cell ( $P < 0.05$ ), which is in agreement with a previous study (27), whereas repression of *FBN1* or *QSCN6* did not affect endothelial cell migration (Fig. 5C). Finally, three-dimensional sprouting of endothelial cell spheroids in a collagen gel was significantly increased by down-regulation of *CLU*, *FBN1*, or *QSCN6* compared with cells transfected with control constructs ( $P < 0.05$ ; Fig. 5D), indicating that these genes are negative regulators in the process of endothelial cell tube formation. Together, these results suggest an inhibitory function for clusterin, fibrillin 1, and quiescin Q6 in endothelial cell growth and sprouting, indicating that the angiostatic activities of DNMT and HDAC inhibitors might be explained by reactivation of angiogenesis-suppressing genes in tumor endothelial cell.

## Discussion

DNMT and HDAC inhibitors induce growth arrest and apoptosis of tumor cells, which is considered to be due to reactivation of epigenetically silenced tumor-suppressor genes (7, 28, 29). Recently, we (12) and others (13, 14) found that DNMT and HDAC inhibitors

are also potent angiostatic agents, inhibiting endothelial cell growth and angiogenesis *in vitro* and *in vivo*. However, very little is known on the mechanisms behind the direct angiostatic effects of these compounds. In addition, in contrast to the extensive knowledge on epigenetic aberrations in tumor cells, there is almost nothing known about the role of epigenetics in regulation of gene expression in endothelial cells during tumor angiogenesis. Some studies associated the angiostatic effects of HDAC inhibitors with down-regulation of angiogenesis-related genes in endothelial cells (14, 30, 31). However, these studies did not investigate the direct effects of these compounds on endothelial cell gene expression; that is, increased promoter histone acetylation and thus transcriptional activation of endothelial cell genes. Furthermore, effects of HDAC inhibitors were not related with epigenetic promoter modifications of endothelial cell genes in these studies.

To identify the mechanism behind the direct inhibition of endothelial cell growth and angiogenesis by DNMT and HDAC inhibitors, we did a comprehensive screen for genes reactivated by these compounds in tumor-conditioned endothelial cells. We combined gene expression microarrays with pharmacologic inhibition of DNMT and HDAC activities to identify genes that are epigenetically repressed in tumor-conditioned endothelial cells, as has been previously done in tumor cells (10, 11). This strategy provided a preliminary mechanism for the direct angiostatic effects of DNMT and HDAC inhibitors and revealed more insight into the epigenetic regulation of tumor angiogenesis. In addition, novel angiogenesis-regulating genes were identified, increasing our knowledge into the transcriptional responses of endothelial cells when exposed to angiogenic growth factors.

Interestingly, microarray analysis revealed a significant over-representation of promoter CpG island-containing genes and identified many genes described to be hypermethylated in tumor cells, suggesting that many of the identified genes can be methylated. However, genomic bisulfite sequencing data suggested that silencing of these genes in tumor-conditioned endothelial cells occurs without promoter DNA methylation. Five of the genes analyzed by bisulfite sequencing (i.e., *ICAM1*, *IGFBP3*, *FBN1*, *TSPAN2*, and *QSCN6*) are described to be silenced in tumor cells by promoter hypermethylation (*ICAM1*, *IGFBP3*, *FBN1*, and *TSPAN2*) at CpGs within the area we analyzed and histone deacetylation (*QSCN6*; refs. 32–35). In addition, *CLU* expression in *HRAS*-transformed rat fibroblasts is regulated by promoter DNA hypermethylation (21). Our bisulfite sequencing results might be explained by the presence of very low methylation levels in endothelial cells, in which case the number of clones sequenced may not be sufficient to detect this. However, methylation in only few clones would not be able to explain the major loss of expression observed for these genes in tumor-conditioned endothelial cells. In addition, promoter methylation of some genes was analyzed by methylation-specific PCR, which is a more sensitive but less comprehensive technique to study DNA methylation. Yet, this approach also did not identify methylation of the examined genes (data not shown). Another possibility is that DNA methylation might occur in enhancers or other transcription regulatory sequences located outside the examined region. For example, hypermethylation of *CLU* was reported within the promoter, but also within a CpG island 14.5 kb upstream of the gene (21). Furthermore, methylation of upstream (transcription) factors might be indirectly responsible for gene silencing. In addition, the sensitivity of the microarray is an important issue, which might not be high enough to identify



methyated genes but instead might be identifying genes with altered histone modifications only.

In contrast to promoter DNA methylation, promoter histone H3 acetylation and H3 lysine 4 methylation patterns of the genes examined correlated with changes in gene expression. These data showed that silencing of genes in tumor-conditioned endothelial cells during angiogenesis occurs in association with promoter histone modifications and not DNA methylation. Furthermore, DNMT and HDAC inhibitors reactivated these genes by reversal of promoter histone modifications. Several studies suggest that CpG methylation is not a primary cause of inactivation of transcription, but maintains long-term silencing of genes that have already been switched off by other mechanisms (36, 37). In contrast, histone deacetylation and loss of H3 lysine 4 methylation are more dynamic epigenetic modifications that are suggested to be more initial events in gene silencing. It is tempting to speculate that down-regulation of growth-inhibiting genes in tumor-conditioned endothelial cells by promoter histone modifications is a reversible phenomenon, whereas many of these genes can be maintained in a permanently silent state in tumor cells by promoter DNA hypermethylation after initial silencing by histone modifications. In relation to this, it is possible that culturing HUVEC for 6 days with angiogenic growth factors is not sufficient to induce irreversible gene silencing by promoter DNA methylation. Therefore, we examined promoter methylation of *CLU*, *FBN1*, *TSPAN2*, and *TNFRSF21* in tumor-conditioned endothelial cells after 3 weeks of activation; however, hardly any methylation was found (Supplementary Data 1). Also, for one gene (*ICAMI*), methylation was studied in the HMEC cell line, as well as in microdissected tumor endothelial cells; however, no increase in the amount of methylated CpGs was observed (Fig. 4B).

Despite absence of promoter DNA hypermethylation, the DNMT inhibitor DAC reactivated genes in tumor-conditioned endothelial cells in correlation with increased promoter histone acetylation and H3 lysine 4 methylation. Reactivation of unmethylated genes by DAC in association with increased histone acetylation and/or H3 lysine 4 methylation has also been described in tumor cells (38–40). This might be attributed to the fact that apart from their methylation ability, DNMTs have additional roles in gene silencing. These enzymes exhibit methylation-independent transcription repressor functions by acting as transcriptional repressors themselves, or by serving as binding scaffolds for histone methyltransferases (41) and HDACs (40, 42, 43). By trapping DNMTs, DAC inhibits both the methylation-dependent as well as the methylation-independent activities of these enzymes. The latter results in reactivation of genes through removal of DNMT-associated histone modifications.

When comparing relative induction of gene expression by treatment with DAC or TSA separately with the combined treatment, no additive or synergistic effect was observed. Furthermore, most genes showed greater relative induction by TSA than by DAC. Only for the imprinted genes *NNAT* and *DMD*, relative induction by DAC was greater than by TSA, which may be due to methylation of these genes at the DNA level. These data suggest that silencing of our candidate genes is predominantly an HDAC-dependent mechanism. In contrast, microarray analysis of the colorectal cancer cell line RKO treated with DAC and TSA identified a group of genes that was unaffected by TSA, up-regulated by DAC, and more strongly induced by the combination treatment, and a second group that was up-regulated by TSA with variable response to DAC (10). This was explained by the presence of promoter hypermethylation in the colorectal cancer cell line in the first group of genes and its absence

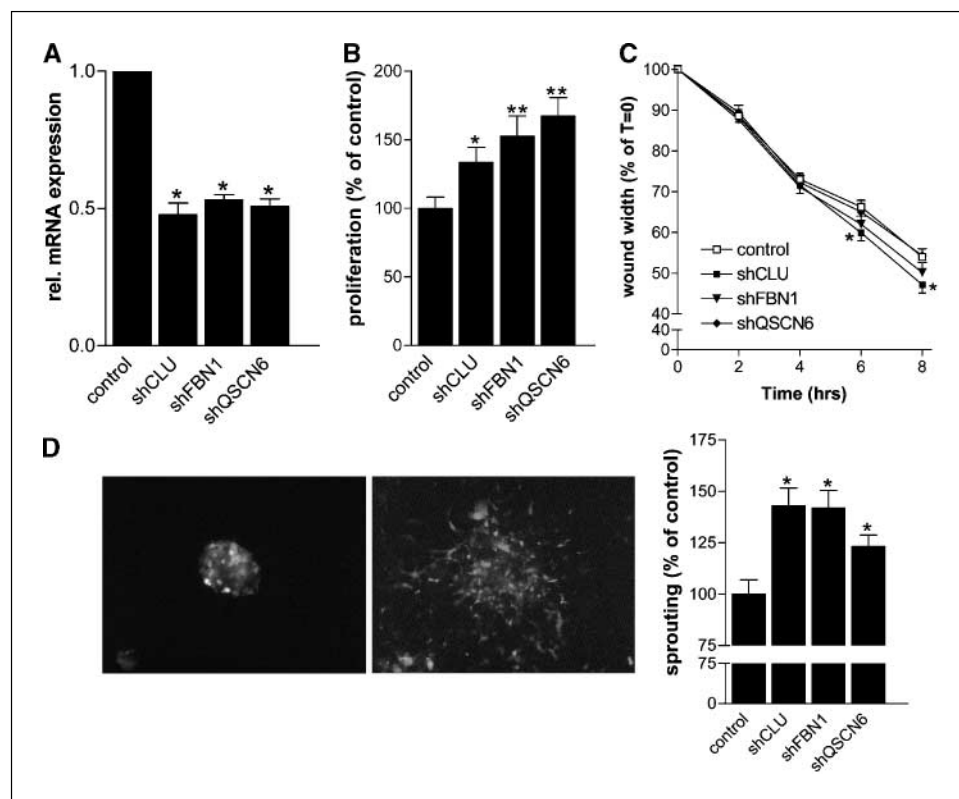


**Figure 5.** Effects of *CLU*, *FBN1*, and *QSCN6* shRNA on endothelial cell proliferation, migration, and sprouting. **A**, relative mRNA expression of *CLU*, *FBN1*, and *QSCN6*, determined by quantitative real-time RT-PCR, 72 h after transfection of HMECs with *CLU*, *FBN1*, *QSCN6*, or control shRNA constructs. Columns, mean of three independent experiments; bars, SE (\*,  $P < 0.05$  versus control). **B**, relative proliferation of HMEC transfected with *CLU*, *FBN1*, *QSCN6*, or control shRNA constructs. Columns, mean of three independent experiments; bars, SE (\*,  $P < 0.05$ , \*\*  $P < 0.01$  versus control). **C**, relative wound width of HMEC monolayers transfected with *CLU*, *FBN1*, *QSCN6*, or control shRNA constructs. Points, mean of three independent experiments; bars, SE (\*,  $P < 0.05$  versus control). **D**, spheroid of HMECs before (left photograph) and after (right photograph) sprouting into a collagen matrix induced by bFGF and VEGF. Tube formation was quantified by taking the relative increase in diameters (measured in two directions) of the spheroids transfected with *CLU*, *FBN1*, *QSCN6*, or control shRNA constructs. Columns, mean of three independent experiments; bars, SE (\*,  $P < 0.05$  versus control).

in the second group. In comparison, most of the genes in this study meet the criteria of up-regulation by TSA with a variable response to DAC in tumor-conditioned endothelial cells, which is reflected by the absence of promoter DNA hypermethylation. A difference between this study and the RKO microarray, however, is that in the latter an initial cDNA subtraction step between mock-treated and DAC- and TSA-treated RKO cells was done to increase the screening sensitivity.

This study identified novel genes functionally involved in angiogenesis. Although complete silencing of mRNA expression was not achieved by shRNA, significant effects on endothelial cell proliferation and angiogenesis were already observed at 50% knockdown of the genes examined. Functional validation revealed that down-regulation of clusterin, fibrillin 1, and quiescin Q6 stimulates growth and sprouting of endothelial cells, whereas repression of clusterin also increases endothelial cell migration. Our findings suggest that clusterin, fibrillin 1, and quiescin Q6 negatively regulate angiogenesis. QSCN6 is proposed to be involved in negative regulation of cell and tissue growth although the exact function is not yet known (44). Clusterin is a widely expressed glycoprotein that has been reported to have both proapoptotic and antiapoptotic functions (45, 46), as well as proangiogenic and antiangiogenic effects (26, 27), which can be explained by functional differences in the various isoforms of the protein and that the function might be context dependent (47). Fibrillin 1, a calcium-binding glycoprotein, is a main structural component of microfibrils situated in the extracellular matrix of connective tissue (48). Deposition of fibrillin by endothelial cell is required for vessel maturation and endothelial cell functioning (49, 50) and thus can be seen as a characteristic of differentiated endothelial cells.

The doses of DAC and TSA used in this study do not induce apoptosis of endothelial cells, as we described previously (12).

Therefore, it is not likely that the toxicity of these compounds is a major cause of gene induction in our microarray. Furthermore, the identification of a significantly high percentage of genes containing promoter CpG islands, and of many genes that have been described to be epigenetically silenced in tumor cells, suggests that we selected for genes prone to silencing by DNMT- and/or HDAC-dependent epigenetic modifications.

In conclusion, this is the first study describing a comprehensive screen for genes reactivated by DNMT and HDAC inhibitors in tumor-conditioned endothelial cells. We identify novel angiogenesis-regulating genes that are down-regulated in activated endothelial cells by promoter histone modifications, and reactivated by DAC and TSA through reversal of epigenetic promoter modifications. Our findings provide a preliminary mechanism for the direct angiostatic effects of DNMT and HDAC inhibitors. Furthermore, this study partly unravels the epigenetic regulation of gene expression in tumor-conditioned endothelial cells during angiogenesis. Although transcriptional repression of six genes was confirmed in tumor-derived endothelial cells, further studies are required to confirm extrapolation of our findings to tumor endothelium *in vivo*. The identification of novel endothelial cell genes with angiogenesis-suppressing activities gives more insight into the biology of tumor angiogenesis. Our findings increase our understanding of, and help in, the future design of epigenetic anticancer therapy.

## Acknowledgments

Received 8/16/2006; revised 2/16/2007; accepted 2/22/2007.

The costs of publication of this article were defrayed in part by the payment of page charges. This article must therefore be hereby marked *advertisement* in accordance with 18 U.S.C. Section 1734 solely to indicate this fact.

We thank Edith van der Linden and Loes van Eijk for assistance with cell culture and Mat Rousch for FACS sorting.

## References

- Carmeliet P. Angiogenesis in life, disease and medicine. *Nature* 2005;438:932–6.
- St Croix B, Rago C, Velculescu V, et al. Genes expressed in human tumor endothelium. *Science* 2000; 289:1197–202.
- Bicknell R, Harris AL. Novel angiogenic signaling pathways and vascular targets. *Annu Rev Pharmacol Toxicol* 2004;44:219–38.
- van Beijnum J, Dings RP, van der Linden E, et al. Gene expression of tumor angiogenesis dissected; specific targeting of colon cancer angiogenic vasculature. *Blood* 2006;108:2339–48.
- Strahl BD, Allis CD. The language of covalent histone modifications. *Nature* 2000;403:41–5.
- Jaenisch R, Bird A. Epigenetic regulation of gene expression: how the genome integrates intrinsic and environmental signals. *Nat Genet* 2003;33 Suppl:245–54.
- Herman JG, Baylin SB. Gene silencing in cancer in association with promoter hypermethylation. *N Engl J Med* 2003;349:2042–54.
- Cameron EE, Bachman KE, Myohanen S, Herman JG, Baylin SB. Synergy of demethylation and histone deacetylase inhibition in the re-expression of genes silenced in cancer. *Nat Genet* 1999;21:103–7.
- Yoo CB, Jones PA. Epigenetic therapy of cancer: past, present and future. *Nat Rev Drug Discov* 2006;5:37–50.
- Suzuki H, Gabrielson E, Chen W, et al. A genomic screen for genes up-regulated by demethylation and histone deacetylase inhibition in human colorectal cancer. *Nat Genet* 2002;31:141–9.
- Yamashita K, Upadhyay S, Osada M, et al. Pharmacologic unmasking of epigenetically silenced tumor suppressor genes in esophageal squamous cell carcinoma. *Cancer Cell* 2002;2:485–95.
- Hellebrekers DM, Jair KW, Vire E, et al. Angiostatic activity of DNA methyltransferase inhibitors. *Mol Cancer Ther* 2006;5:467–75.
- Kim MS, Kwon HJ, Lee YM, et al. Histone deacetylases induce angiogenesis by negative regulation of tumor suppressor genes. *Nat Med* 2001;7:437–43.
- Deroanne CF, Bonjean K, Servotte S, et al. Histone deacetylase inhibitors as anti-angiogenic agents altering vascular endothelial growth factor signaling. *Oncogene* 2002;21:427–36.
- van der Schaft DW, Toebes EA, Haseman JR, Mayo KH, Griffioen AW. Bactericidal/permeability-increasing protein (BPI) inhibits angiogenesis via induction of apoptosis in vascular endothelial cells. *Blood* 2000;96: 176–81.
- Thijssen VL, Brandwijk RJ, Dings RP, Griffioen AW. Angiogenesis gene expression profiling in xenograft models to study cellular interactions. *Exp Cell Res* 2004; 299:286–93.
- Metivier R, Penot G, Hubner MR, et al. Estrogen receptor- $\alpha$  directs ordered, cyclical, and combinatorial recruitment of cofactors on a natural target promoter. *Cell* 2003;115:751–63.
- van der Schaft DW, Dings RP, de Lussanet QG, et al. The designer anti-angiogenic peptide anginex targets tumor endothelial cells and inhibits tumor growth in animal models. *FASEB J* 2002;16:1991–3.
- Gardiner-Garden M, Frommer M. CpG islands in vertebrate genomes. *J Mol Biol* 1987;196:261–82.
- Cross SH, Charlton JA, Nan X, Bird AP. Purification of CpG islands using a methylated DNA binding column. *Nat Genet* 1994;6:236–44.
- Lund P, Weissaupt K, Mikeska T, et al. Oncogenic HRAS suppresses clusterin expression through promoter hypermethylation. *Oncogene* 2006;25:4890–903.
- Chan GC, Fish JE, Mawji IA, Leung DD, Rachlis AC, Marsden PA. Epigenetic basis for the transcriptional hyporesponsiveness of the human inducible nitric oxide synthase gene in vascular endothelial cells. *J Immunol* 2005;175:3846–61.
- Franklin SL, Ferry RJ, Jr., Cohen P. Rapid insulin-like growth factor (IGF)-independent effects of IGF binding protein-3 on endothelial cell survival. *J Clin Endocrinol Metab* 2003;88:900–7.
- Iwatsuki K, Tanaka K, Kaneko T, et al. Runx1 promotes angiogenesis by downregulation of insulin-like growth factor-binding protein-3. *Oncogene* 2004;24:1129–37.
- Griffioen AW, Damen CA, Martinotti S, Blijham GH, Groenewegen G. Endothelial intercellular adhesion molecule-1 expression is suppressed in human malignancies: the role of angiogenic factors. *Cancer Res* 1996; 56:1111–7.
- Jackson JK, Gleave ME, Gleave J, Burt HM. The inhibition of angiogenesis by antisense oligonucleotides to clusterin. *Angiogenesis* 2005;8:229–38.
- Sivamurthy N, Stone DH, LoGerfo FW, Quist WC. Apolipoprotein J inhibits the migration and adhesion of endothelial cells. *Surgery* 2001;130:204–9.
- Bender CM, Pao MM, Jones PA. Inhibition of DNA methylation by 5-aza-2'-deoxycytidine suppresses the growth of human tumor cell lines. *Cancer Res* 1998;58: 95–101.
- Marks PA, Richon VM, Kelly WK, Chiao JH, Miller T. Histone deacetylase inhibitors: development as cancer therapy. *Novartis Found Symp* 2004;259:269–81; discussion 81–8.

30. Qian DZ, Wang X, Kachhap SK, et al. The histone deacetylase inhibitor NVP-LAQ824 inhibits angiogenesis and has a greater antitumor effect in combination with the vascular endothelial growth factor receptor tyrosine kinase inhibitor PTK787/ZK222584. *Cancer Res* 2004;64:6626-34.
31. Rossig L, Li H, Fisslthaler B, et al. Inhibitors of histone deacetylation downregulate the expression of endothelial nitric oxide synthase and compromise endothelial cell function in vasorelaxation and angiogenesis. *Circ Res* 2002;91:837-44.
32. Friedrich MG, Chandrasoma S, Siegmund KD, et al. Prognostic relevance of methylation markers in patients with non-muscle invasive bladder carcinoma. *Eur J Cancer* 2005;41:2769-78.
33. Chang YS, Wang L, Liu D, et al. Correlation between insulin-like growth factor-binding protein-3 promoter methylation and prognosis of patients with stage I non-small cell lung cancer. *Clin Cancer Res* 2002;8:3669-75.
34. Miyamoto K, Fukutomi T, Akashi-Tanaka S, et al. Identification of 20 genes aberrantly methylated in human breast cancers. *Int J Cancer* 2005;116:407-14.
35. Chiba T, Yokosuka O, Fukai K, et al. Cell growth inhibition and gene expression induced by the histone deacetylase inhibitor, trichostatin A, on human hepatoma cells. *Oncology* 2004;66:481-91.
36. Tamaru H, Selker EU. A histone H3 methyltransferase controls DNA methylation in *Neurospora crassa*. *Nature* 2001;414:277-83.
37. Bachman KE, Park BH, Rhee I, et al. Histone modifications and silencing prior to DNA methylation of a tumor suppressor gene. *Cancer Cell* 2003;3:89-95.
38. Nguyen CT, Weisenberger DJ, Velicescu M, et al. Histone H3-lysine 9 methylation is associated with aberrant gene silencing in cancer cells and is rapidly reversed by 5-aza-2'-deoxycytidine. *Cancer Res* 2002;62:6456-61.
39. Schmelz K, Sattler N, Wagner M, Lubbert M, Dorken B, Tamm I. Induction of gene expression by 5-Aza-2'-deoxycytidine in acute myeloid leukemia (AML) and myelodysplastic syndrome (MDS) but not epithelial cells by DNA-methylation-dependent and -independent mechanisms. *Leukemia* 2005;19:103-11.
40. Fuks F, Burgers WA, Brehm A, Hughes-Davies L, Kouzarides T. DNA methyltransferase Dnmt1 associates with histone deacetylase activity. *Nat Genet* 2000;24:88-91.
41. Lehnertz B, Ueda Y, Derijck AA, et al. Suv39h-mediated histone H3 lysine 9 methylation directs DNA methylation to major satellite repeats at pericentric heterochromatin. *Curr Biol* 2003;13:1192-200.
42. Robertson KD, Ait-Si-Ali S, Yokochi T, Wade PA, Jones PL, Wolffe AP. DNMT1 forms a complex with Rb, E2F1 and HDAC1 and represses transcription from E2F-responsive promoters. *Nat Genet* 2000;25:338-42.
43. Rountree MR, Bachman KE, Baylin SB. DNMT1 binds HDAC2 and a new co-repressor, DMAP1, to form a complex at replication foci. *Nat Genet* 2000;25:269-77.
44. Coppock DL, Cina-Poppe D, Gilleran S. The quiescin Q6 gene (QSCN6) is a fusion of two ancient gene families: thioredoxin and ERV1. *Genomics* 1998;54:460-8.
45. Chen T, Turner J, McCarthy S, Scaltriti M, Bettuzzi S, Yeatman TJ. Clusterin-mediated apoptosis is regulated by adenomatous polyposis coli and is p21 dependent but p53 independent. *Cancer Res* 2004;64:7412-9.
46. Zhang H, Kim JK, Edwards CA, Xu Z, Taichman R, Wang CY. Clusterin inhibits apoptosis by interacting with activated Bax. *Nat Cell Biol* 2005;7:909-15.
47. Leskov KS, Klovov DY, Li J, Kinsella TJ, Boothman DA. Synthesis and functional analyses of nuclear clusterin, a cell death protein. *J Biol Chem* 2003;278:11590-600.
48. Handford PA. Fibrillin-1, a calcium binding protein of extracellular matrix. *Biochim Biophys Acta* 2000;1498:84-90.
49. Carta L, Pereira L, Arteaga-Solis E, et al. Fibrillins 1 and 2 perform partially overlapping functions during aortic development. *J Biol Chem* 2006;281:8016-23.
50. Wilson DG, Bellamy MF, Ramsey MW, et al. Endothelial function in Marfan syndrome: selective impairment of flow-mediated vasodilation. *Circulation* 1999;99:909-15.

## Identification of Epigenetically Silenced Genes in Tumor Endothelial Cells

Debby M.E.I. Hellebrekers, Veerle Melotte, Emmanuelle Viré, et al.

*Cancer Res* 2007;67:4138-4148.

<b>Updated version</b>	Access the most recent version of this article at: <a href="http://cancerres.aacrjournals.org/content/67/9/4138">http://cancerres.aacrjournals.org/content/67/9/4138</a>
<b>Supplementary Material</b>	Access the most recent supplemental material at: <a href="http://cancerres.aacrjournals.org/content/suppl/2007/04/26/67.9.4138.DC1">http://cancerres.aacrjournals.org/content/suppl/2007/04/26/67.9.4138.DC1</a>

<b>Cited articles</b>	This article cites 50 articles, 16 of which you can access for free at: <a href="http://cancerres.aacrjournals.org/content/67/9/4138.full.html#ref-list-1">http://cancerres.aacrjournals.org/content/67/9/4138.full.html#ref-list-1</a>
<b>Citing articles</b>	This article has been cited by 18 HighWire-hosted articles. Access the articles at: <a href="/content/67/9/4138.full.html#related-urls">/content/67/9/4138.full.html#related-urls</a>

<b>E-mail alerts</b>	<a href="#">Sign up to receive free email-alerts</a> related to this article or journal.
<b>Reprints and Subscriptions</b>	To order reprints of this article or to subscribe to the journal, contact the AACR Publications Department at <a href="mailto:pubs@aacr.org">pubs@aacr.org</a> .
<b>Permissions</b>	To request permission to re-use all or part of this article, contact the AACR Publications Department at <a href="mailto:permissions@aacr.org">permissions@aacr.org</a> .